



Rotating Hydromagnetic Two-Fluid Convective Flow and Temperature Distribution in an Inclined Channel

P. Sri Ramachandra Murty^{1*}, G. Balaji Prakash², Ch. Karuna Sree³

¹Department of Mathematics, GIT, GITAM (Deemed to be University), Visakhapatnam-530 045, A.P., India.

²Department of Mathematics, K.L.E.F. (Deemed to be University), Guntur, A.P., India.

³Department of Mathematics, VFSTR (Deemed to be University), Vadlamudi, Guntur, A.P., India.

*Corresponding author E-mail: drmurtypr@gmail.com

Abstract

Magnetohydrodynamic convective two-fluid flow and temperature distribution between two inclined parallel plates in which one fluid being electrically non-conducting and the other fluid is electrically conducting is studied. A constant magnetic field is applied normal to the flow. The system is rotated about y-axis with an angular velocity ‘ Ω ’. Perturbation method is used to obtain solutions for primary velocity, secondary velocity and temperature distribution by assuming that the fluids in the two regions are incompressible, laminar, steady and fully developed. Increasing values of rotation is to reduce temperature distribution and primary velocity where as the secondary velocity increases for smaller rotation, while for larger rotation it decreases.

Keywords: Two fluid flow; inclined channel; magnetohydrodynamics.

1. Introduction

Temperature distribution in convective Hartmann flow in a horizontal channel has been studied extensively for decades. Shail [1] analyzed the two-phase flow between two insulated plates in which one-phase being electrically non-conducting. Seth et. al. [2] presented the rotating Hartmann flow in the presence of inclined magnetic field. Lohrasbi and Sahai [3] discussed magnetohydrodynamic two-phase flow with temperature distribution in a horizontal channel. Two-phase hydromagnetic flow and heat transfer in a horizontal channel is investigated analytically by Malashetty and Leela [4]. Raju and Murty [5] analyzed rotating MHD two-phase flow and temperature distribution in a horizontal channel. Chauhan and Rastogi [6] considered the heat transfer aspects on rotating couette flow through porous medium. Abdul Mateen [7, 8] has studied the magnetohydrodynamic flow and transient magnetohydrodynamic flow of two immiscible fluids in a horizontal channel. In the study of heat transfer aspects like solar collector technology, inclined geometry has enormous applications. But considerable attention has not been taken on these problems except the studies by Malashetty and Umavathi [9], Malashetty et. al. [10], Simon Daniel and Shagaiya Daniel [11] and Murty and Balaji [12, 13, 14]. In the present problem, rotating hydromagnetic two fluid flow and temperature distribution through two inclined parallel plates in which one-phase being electrically non-conducting and the other phase is electrically conducting is studied.

2. Formulation of the Problem

Magnetohydrodynamic two-fluid flow driven by a pressure gradient $(-\partial p/\partial x)$ in an inclined channel consisting of two infinite

parallel plates making an angle ϕ with the horizontal plane has been considered. A uniform magnetic field B_0 is applied in the y-direction. The system is rotated with an angular velocity Ω normal to the plates. Figure 1 illustrates the physical configuration of the problem. The fluid in the region $0 \leq y \leq h_1$ is electrically non-conducting and the fluid in the region $-h_2 \leq y \leq 0$ is electrically conducting. The transport properties of the two fluids are taken to be constant. The fluids in both the phases are assumed to be incompressible with different densities, thermal conductivities and viscosities.

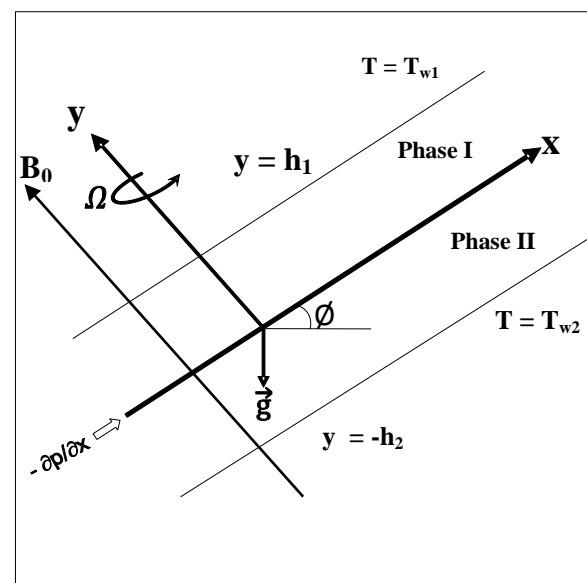


Fig. 1: Physical configuration

With these assumptions, the equations of energy and motion for Boussinesq fluid as in Malashetty and Umavathi [9] for both phases are:

Phase-I

$$\begin{aligned} \mu_1 \frac{d^2 u_1}{dy^2} + \rho_1 g \beta_1 \sin \phi (T_1 - T_{w2}) &= \frac{\partial p}{\partial x} + 2\rho_1 \Omega w_1, \\ \mu_1 \frac{d^2 w_1}{dy^2} &= -2\rho_1 \Omega u_1, \\ \frac{d^2 T_1}{dy^2} + \frac{\mu_1}{K_1} \left[\left(\frac{du_1}{dy} \right)^2 + \left(\frac{dw_1}{dy} \right)^2 \right] &= 0. \end{aligned} \quad (1)$$

Phase-II

$$\begin{aligned} \mu_2 \frac{d^2 u_2}{dy^2} + \rho_2 g \beta_2 \sin \phi (T_2 - T_{w2}) - \sigma B_0^2 u_2 &= \frac{\partial p}{\partial x} + 2\rho_2 \Omega w_2, \\ \mu_2 \frac{d^2 w_2}{dy^2} - \sigma B_0^2 w_2 &= -2\rho_2 \Omega u_2, \\ \frac{d^2 T_2}{dy^2} + \frac{\mu_2}{K_2} \left[\left(\frac{du_2}{dy} \right)^2 + \left(\frac{dw_2}{dy} \right)^2 \right] + \frac{\sigma B_0^2}{K_2} (u_2^2 + w_2^2) &= 0. \end{aligned} \quad (2)$$

Here u_i and w_i are the primary and secondary velocity distributions along x and z -directions respectively, β_i is the coefficient of thermal expansion and T_i is the temperature. The no-slip condition requires that the velocity must be vanishing at the wall. The boundary and interface conditions on primary and secondary velocity distributions are:

$$u_1(h_1) = 0, w_1(h_1) = 0; u_1(0) = u_2(0),$$

$$u_2(-h_2) = 0, w_2(-h_2) = 0; w_1(0) = w_2(0)$$

$$\mu_1 \frac{du_1}{dy} = \mu_2 \frac{du_2}{dy} \text{ and } \mu_1 \frac{dw_1}{dy} = \mu_2 \frac{dw_2}{dy} \text{ at } y = 0. \quad (3)$$

Since the walls are maintained at different temperatures T_{w1} and T_{w2} , the boundary conditions on T_1 and T_2 are given by:

$$\begin{aligned} T_1(h_1) &= T_{w1}, T_1(0) = T_2(0), T_2(-h_2) = T_{w2}, \\ K_1 \frac{dT_1}{dy} &= K_2 \frac{dT_2}{dy} \text{ at } y = 0. \end{aligned} \quad (4)$$

In making these equations dimensionless, the following transformations are used

$$\begin{aligned} u_1^* &= \frac{u_1}{u_1}, \quad u_2^* = \frac{u_2}{u_1}, \quad w_1^* = \frac{w_1}{u_1}, \quad w_2^* = \frac{w_2}{u_1}, \quad y_1^* = \frac{y_1}{h_1}, \\ y_2^* &= \frac{y_2}{h_2}, \quad \theta = \frac{(T - T_{w2})}{(T_{w1} - T_{w2})}, \quad \text{Re} = \frac{\bar{u}_1 h_1}{\nu_1}, \quad b = \frac{\beta_2}{\beta_1}, \\ Gr &= \frac{g \beta_1 h_1^3 (T_{w1} - T_{w2})}{\nu_1^2}, \quad R^2 = \frac{\Omega h_1^2}{\nu}, \quad K = \frac{K_1}{K_2}, \quad h = \frac{h_2}{h_1}, \end{aligned}$$

$$\begin{aligned} n &= \frac{\rho_2}{\rho_1}, \quad M = B_0 h_2 \sqrt{\frac{\sigma}{\mu_2}}, \quad \text{Pr} = \frac{\mu_1 C_p}{K_1}, \quad P = \left(\frac{h_1^2}{\mu_1 \bar{u}_1} \right) \left(\frac{\partial p}{\partial x} \right), \\ Ec &= \frac{\bar{u}_1^2}{C_p (T_{w1} - T_{w2})}, \quad m = \frac{\mu_1}{\mu_2}. \end{aligned} \quad (5)$$

Here Re is the Reynolds number, Ec is the Eckert number, M is the Hartmann number, Pr is the Prandtl number, Gr is the Grashof number, P is the non-dimensional pressure gradient and \bar{u}_1 is the average velocity.

Using the above transformations, the equations (1) and (2) become:

Phase-I

$$\begin{aligned} \frac{d^2 u_1}{dy^2} + \frac{Gr}{\text{Re}} \sin \phi \theta_1 &= P + 2R^2 w_1, \\ \frac{d^2 w_1}{dy^2} &= -2R^2 u_1, \\ \frac{d^2 \theta_1}{dy^2} + \text{Pr} Ec \left[\left(\frac{du_1}{dy} \right)^2 + \left(\frac{dw_1}{dy} \right)^2 \right] &= 0. \end{aligned} \quad (6)$$

Phase-II

$$\begin{aligned} \frac{d^2 u_2}{dy^2} + \frac{Gr}{\text{Re}} A \sin \phi \theta_2 - M^2 u_2 &= CP + 2R^2 w_2, \\ \frac{d^2 w_2}{dy^2} - M^2 w_2 &= -2R^2 u_2, \\ \frac{d^2 \theta_2}{dy^2} + \text{Pr} Ec D \left[\left(\frac{du_2}{dy} \right)^2 + \left(\frac{dw_2}{dy} \right)^2 \right] &+ \text{Pr} Ec D M^2 (u_2^2 + w_2^2) = 0. \end{aligned} \quad (7)$$

The non-dimensional forms of the boundary and interface conditions (3) and (4) become:

$$u_1(1) = 0, w_1(1) = 0, u_1(0) = u_2(0), w_1(0) = w_2(0), u_2(-1) = 0,$$

$$w_2(-1) = 0, \frac{du_1}{dy} = \frac{1}{mh} \frac{du_2}{dy} \text{ and } \frac{dw_1}{dy} = \frac{1}{mh} \frac{dw_2}{dy} \text{ at } y = 0,$$

$$\begin{aligned} \theta_1(1) &= 1, \theta_1(0) = \theta_2(0), \theta_2(-1) = 0, \\ \frac{d\theta_1}{dy} &= \frac{1}{Kh} \frac{d\theta_2}{dy} \text{ at } y = 0. \end{aligned} \quad (8)$$

Writing $q_1 = u_1 + iw_1$ and $q_2 = u_2 + iw_2$, equations (6) and (7) can be written in complex form as:

Phase-I

$$\begin{aligned} \frac{d^2 q_1}{dy^2} + \frac{Gr}{\text{Re}} \sin \phi \theta_1 &= P - 2iR^2 q_1, \\ \frac{d^2 \theta_1}{dy^2} + \text{Pr} Ec \left[\frac{dq_1}{dy} \frac{d\bar{q}_1}{dy} \right] &= 0. \end{aligned} \quad (9)$$

Phase-II

$$\frac{d^2 q_2}{dy^2} + \frac{Gr}{\text{Re}} A \sin \phi \theta_2 - M^2 q_2 = CP - 2iR^2 q_2,$$

$$\frac{d^2\theta_2}{dy^2} + PrEcD \left[\frac{dq_2}{dy} \frac{d\bar{q}_2}{dy} \right] + PrEcDM^2(q_2\bar{q}_2) = 0 \quad (10)$$

The corresponding boundary and interface conditions are:

$$\begin{aligned} q_1(1) = 0, \quad q_1(0) = q_2(0), \quad q_2(-1) = 0, \\ \frac{dq_1}{dy} = \frac{1}{mh} \frac{dq_2}{dy} \text{ at } y = 0, \\ \theta_1(1) = 1, \quad \theta_1(0) = \theta_2(0), \quad \theta_2(-1) = 0, \\ \frac{d\theta_1}{dy} = \frac{1}{Kh} \frac{d\theta_2}{dy} \text{ at } y = 0. \end{aligned} \quad (11)$$

3. Solutions of the Problem

The governing equations are coupled and non-linear. Here, we consider the Eckert number Ec as very small. Hence, Pr.Ec (=ε) is also small and is used in the perturbation method. The solutions are considered in the form

$$(q_i, \theta_i) = (q_{i0}, \theta_{i0}) + \varepsilon(q_{i1}, \theta_{i1}) + \dots \quad (12)$$

where q_{i0}, θ_{i0} are solutions for the case ε equal to zero and q_{i1}, θ_{i1} are perturbed quantities related to q_{i0}, θ_{i0} respectively. Substituting the above solutions in equations (9) and (10) and equating the coefficients of similar powers of ε, we get equations of zeroth-order and first-order approximations for Phase I and Phase II as follows:

Phase I

Equations of zeroth-order approximation:

$$\begin{aligned} \frac{d^2q_{10}}{dy^2} + \frac{Gr}{Re} \sin\phi \theta_{10} = P - 2iR^2q_{10}, \\ \frac{d^2\theta_{10}}{dy^2} = 0. \end{aligned} \quad (13)$$

Equations of first-order approximation:

$$\begin{aligned} \frac{d^2q_{11}}{dy^2} + \frac{Gr}{Re} \sin\phi \theta_{11} = -2iR^2q_{11}, \\ \frac{d^2\theta_{11}}{dy^2} + \left[\frac{dq_{10}}{dy} \frac{d\bar{q}_{10}}{dy} \right] = 0. \end{aligned} \quad (14)$$

Phase-II

Equations of zeroth-order approximation:

$$\begin{aligned} \frac{d^2q_{20}}{dy^2} + \frac{Gr}{Re} A \sin\phi \theta_{20} - M^2q_{20} = CP - 2iR^2q_{20}, \\ \frac{d^2\theta_{20}}{dy^2} = 0 \end{aligned} \quad (15)$$

Equations of first-order approximation:

$$\begin{aligned} \frac{d^2q_{21}}{dy^2} + \frac{Gr}{Re} A \sin\phi \theta_{21} - M^2q_{21} = -2iR^2q_{21} \\ \frac{d^2\theta_{21}}{dy^2} + D \left[\frac{dq_{20}}{dy} \frac{d\bar{q}_{20}}{dy} \right] + DM^2[q_{20}\bar{q}_{20}] = 0. \end{aligned} \quad (16)$$

The corresponding boundary conditions given in equation (11) reduce to:

$$\begin{aligned} q_{10}(1) = 0, \quad q_{10}(0) = q_{20}(0), \quad q_{20}(-1) = 0, \\ \frac{dq_{10}}{dy} = \frac{1}{mh} \frac{dq_{20}}{dy} \text{ at } y = 0, \\ \theta_{10}(1) = 1, \quad \theta_{10}(0) = \theta_{20}(0), \quad \theta_{20}(-1) = 0, \\ \frac{d\theta_{10}}{dy} = \frac{1}{Kh} \frac{d\theta_{20}}{dy} \text{ at } y = 0. \end{aligned} \quad (17)$$

$$\begin{aligned} q_{11}(1) = 0, \quad q_{11}(0) = q_{21}(0), \quad q_{21}(-1) = 0, \\ \frac{dq_{11}}{dy} = \frac{1}{mh} \frac{dq_{21}}{dy} \text{ at } y = 0, \\ \theta_{11}(1) = 0, \quad \theta_{11}(0) = \theta_{21}(0), \quad \theta_{21}(-1) = 0, \\ \frac{d\theta_{11}}{dy} = \frac{1}{Kh} \frac{d\theta_{21}}{dy} \text{ at } y = 0. \end{aligned} \quad (18)$$

It is noted that

$$\begin{aligned} q_{10} = u_{10} + i w_{10}, \quad q_{20} = u_{20} + i w_{20}, \\ q_{11} = u_{11} + i w_{11} \text{ and } q_{21} = u_{21} + i w_{21}. \end{aligned}$$

Solutions for the equations of zeroth-order approximations (13) and (15) using boundary conditions (17) are:

$$\begin{aligned} \theta_{10} = \frac{y + Kh}{1 + Kh}, \quad \theta_{20} = \frac{Kh(1 + y)}{1 + Kh} \\ u_{10} = (c_1 e^{a_6 y} + c_2 e^{-a_6 y}) \cos a_6 y, \\ u_{20} = (c_3 e^{a_16 y} + c_4 e^{-a_16 y}) \cos a_{17} y + a_{23} + a_{25} y, \\ w_{10} = (c_2 e^{-a_6 y} - c_1 e^{a_6 y}) \sin a_6 y + (a_8 y + a_7), \\ w_{20} = (c_4 e^{-a_16 y} - c_3 e^{a_16 y}) \sin a_{17} y + a_{24} + a_{26} y \end{aligned} \quad (19)$$

Solutions for the equations of first-order approximations (14) and (16) using boundary conditions (18) are:

$$\begin{aligned} \theta_{11} = \{c_5 y + c_6 - a_{89} e^{2a_6 y} - a_{90} \cos 2a_6 y - a_{91} e^{-2a_6 y} + \\ a_{92} e^{-a_6 y} \sin a_6 y + a_{92} e^{-a_6 y} \cos a_6 y + a_{93} e^{a_6 y} \sin a_6 y \\ - a_{93} e^{a_6 y} \cos a_6 y - a_{94} y^2\} \\ - i \{a_{95} e^{a_6 y} \sin a_6 y + a_{95} e^{a_6 y} \cos a_6 y - a_{96} e^{-a_6 y} \sin a_6 y \\ + a_{96} e^{-a_6 y} \cos a_6 y - a_{308} \sin 2a_6 y\}, \\ \theta_{21} = \{c_7 y + c_8 - a_{174} e^{2a_{16} y} + a_{175} \cos 2a_{17} y \\ - a_{176} e^{-2a_{16} y} - a_{242} e^{a_{16} y} \cos a_{17} y \\ - a_{243} e^{a_{16} y} \sin a_{17} y - a_{244} e^{-a_{16} y} \cos a_{17} y \\ - a_{245} e^{-a_{16} y} \sin a_{17} y - a_{246} e^{a_{16} y} y \cos a_{17} y \\ - a_{247} e^{a_{16} y} y \sin a_{17} y - a_{248} e^{-a_{16} y} y \cos a_{17} y \\ - a_{249} e^{-a_{16} y} y \sin a_{17} y - a_{214} y^4 \\ - a_{215} y^3 - a_{216} y^2\} \\ + i \{a_{217} \sin 2a_{17} y - a_{250} e^{a_{16} y} \sin a_{17} y \\ - a_{251} e^{a_{16} y} \cos a_{17} y - a_{252} e^{-a_{16} y} \sin a_{17} y \\ - a_{253} e^{-a_{16} y} \cos a_{17} y - a_{254} e^{a_{16} y} y \cos a_{17} y \\ - a_{255} e^{a_{16} y} y \sin a_{17} y - a_{256} e^{-a_{16} y} y \cos a_{17} y \\ - a_{257} e^{-a_{16} y} y \sin a_{17} y\}, \end{aligned}$$

$$\begin{aligned}
u_{11} &= (c_9 e^{a_6 y} + c_{10} e^{-a_6 y}) \cos a_6 y \\
&+ b_{17} e^{2a_6 y} + b_{18} e^{-2a_6 y} + b_{19} \cos 2a_6 y \\
&+ b_{20} \sin 2a_6 y - b_{21} e^{-a_6 y} y \cos a_6 y \\
&- b_{22} e^{a_6 y} y \cos a_6 y + b_{23}, \\
w_{11} &= (c_{10} e^{-a_6 y} - c_9 e^{a_6 y}) \sin a_6 y \\
&- b_{24} e^{2a_6 y} - b_{25} e^{-2a_6 y} + b_{26} \cos 2a_6 y \\
&- b_{27} \sin 2a_6 y - b_{28} e^{a_6 y} y \sin a_6 y \\
&- b_{29} e^{-a_6 y} y \sin a_6 y - b_{30} y^2 \\
&+ b_{31} y + b_{32}, \\
u_{21} &= (c_{11} e^{a_{16} y} + c_{12} e^{-a_{16} y}) \cos a_{17} y \\
&+ b_{124} e^{2a_{16} y} + b_{125} e^{-2a_{16} y} + b_{126} \cos 2a_{17} y \\
&- b_{127} \sin 2a_{17} y - b_{128} e^{a_{16} y} y \sin a_{17} y \\
&- b_{129} e^{-a_{16} y} y \cos a_{17} y - b_{130} e^{-a_{16} y} y \sin a_{17} y \\
&- b_{131} e^{-a_{16} y} y \cos a_{17} y - b_{132} e^{a_{16} y} y^2 \sin a_{17} y \\
&- b_{133} e^{a_{16} y} y^2 \cos a_{17} y - b_{134} e^{-a_{16} y} y^2 \sin a_{17} y \\
&- b_{135} e^{-a_{16} y} y^2 \cos a_{17} y - b_{136} y^4 - b_{137} y^3 \\
&- b_{138} y^2 - b_{139} y - b_{140}, \\
w_{21} &= (c_{12} e^{-a_{16} y} - c_{11} e^{a_{16} y}) \sin a_{17} y \\
&- b_{141} e^{2a_{16} y} - b_{142} e^{-2a_{16} y} + b_{143} \cos 2a_{17} y \\
&+ b_{144} \sin 2a_{17} y - b_{147} e^{-a_{16} y} y \cos a_{17} y \\
&- b_{148} e^{-a_{16} y} y \sin a_{17} y - b_{149} e^{a_{16} y} y^2 \sin a_{17} y \\
&- b_{150} e^{a_{16} y} y^2 \cos a_{17} y - b_{151} e^{-a_{16} y} y^2 \sin a_{17} y \\
&- b_{152} e^{-a_{16} y} y^2 \cos a_{17} y - b_{153} y^4 - b_{154} y^3 \\
&- b_{155} y^2 - b_{156} y - b_{157}. \tag{20}
\end{aligned}$$

The constants involved in the equations (19) and (20) are not given for the sake of brevity. Solutions for the equations zeroth-order and first-order approximations (13) - (16) are solved numerically by fixing the parameters $n = 1.5$, $Re = 5$, $K = 1$, $b = 1$ and $P = -5$. As the solutions for the equations of zeroth-order approximation are linear, the graphs for temperature distribution are drawn only for first order approximations. This show that the temperature distribution up to zeroth-order approximation is due to the conduction only. In figures 2 – 18, except the varying one, all other parameters are chosen from the set $(\phi, h, Gr, R, m, M) = (30, 1, 5, 1, 0.5, 2)$.

4. Results and Discussion

Approximate solutions for primary velocity, secondary velocity and temperature distribution are obtained by solving the resulting differential equations analytically. Numerical values of these solutions are computed for various sets of the parameters and the results are represented graphically. Here we note that, when the rotation $R=0$, these results are in agreement with that of Malashetty and Umavathi [9].

Primary velocity distribution u and secondary velocity distribution w for various values of the rotation parameter R are shown in figures 2 and 3, respectively. It is concluded that 'u' reduces with increasing rotation. Since R is the ratio of the Coriolis force and

the viscous force, as R increases the Coriolis force also increases. The increasing Coriolis forces oppose the buoyancy force. Hence the velocity will be decreased. It is also concluded that as the rotation parameter R increases in $(0, 1.6)$, the secondary velocity w also increases, but outside the range as R increases, it decreases. The effect of the Hartmann number M on 'u' and 'w' is shown in figures 4 and 5, respectively. As M increases both the velocities decrease. This is because, increasing Hartmann number causes greater interaction between the magnetic field and the fluid motion and that increases the Lorentz force. Since the Lorentz force opposes the buoyancy force, both the velocities will be reduced. Figures 6 and 7 represent 'u' and 'w' for different values of the Grashof number Gr . As Gr increases, both the velocities also increase. The effect of the ratio of heights h on 'u' and 'w' is shown in figures 8 and 9, respectively. The effect of increasing h is to enhance both the velocities. The effect of the angle of inclination ϕ on 'u' and 'w' is shown in figures 10 and 11, respectively. As the buoyancy force enhances with increase in the inclination angle, both the primary and secondary velocities increase with the increasing values of ϕ . Figures 12 and 13 show the effect of the ratio of viscosities m on primary and secondary velocities respectively. The effect of increasing m is to increase both primary and secondary velocities.

Figure 14 represents the effect of R on temperature distribution θ . It is observed that the temperature reduces with increasing rotation. The effect of Hartmann number M on temperature distribution θ is represented in figure 15. It is noticed that the temperature decreases with increasing values of M . Figure 16 shows the effect of Gr on temperature θ . We observe that the temperature increases with the increasing values of Gr . Figure 17 shows the effect of the ratio of viscosities m on the temperature distribution. Increasing values of m enhances the temperature of the flow. The effect of the angle of inclination ϕ on temperature θ is represented in figure 18. Increasing values of ϕ enhances the temperature. This is because, as ϕ increases the buoyancy force also increases which enhances the temperature.

5. Conclusions

This problem is concerned with the analysis of rotating hydromagnetic two-fluid flow and temperature distribution in an inclined channel containing electrically conducting fluid superposed by the electrically non-conducting fluid. Perturbation method is used to obtain approximate solutions for primary velocity, secondary velocity and temperature distribution. The important conclusions from this study are:

- It is observed that electrically non-conducting fluid generates less heat than electrically conducting fluid due to diffusion.
- The increasing rotation parameter is to reduce the temperature and primary velocity of the flow in both the regions.
- The increasing Hartmann number is to reduce the temperature, secondary velocity and primary velocity in both the phases. This is because, the drag caused by the effect of the Hartmann number on the flow of the second phase also effects the flow of the first phase (electrically non-conducting fluid). Hence there is substantial effect of Hartmann number on the first phase also.
- Increasing values of inclination angle, Grashof number, ratio of viscosities of two fluids is for enhancing the temperature, primary and secondary velocities of the flow in the two regions.

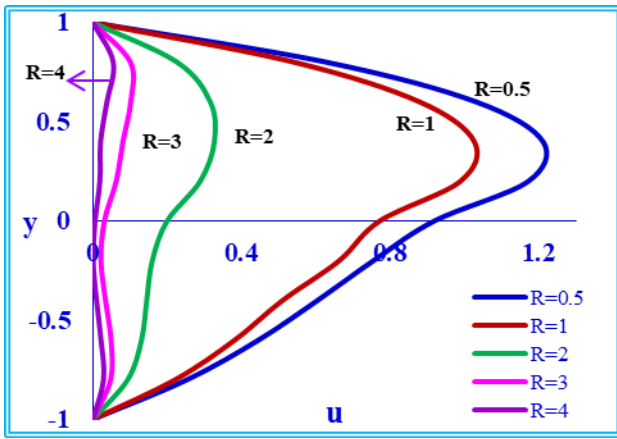


Fig.2: Primary velocity for various values of R.

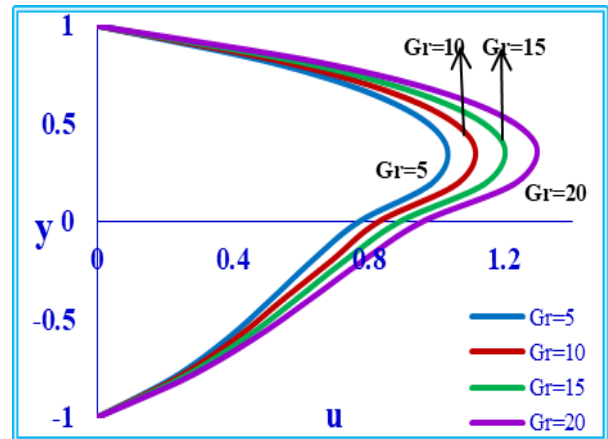


Fig. 6: Primary velocity for various values of Gr.

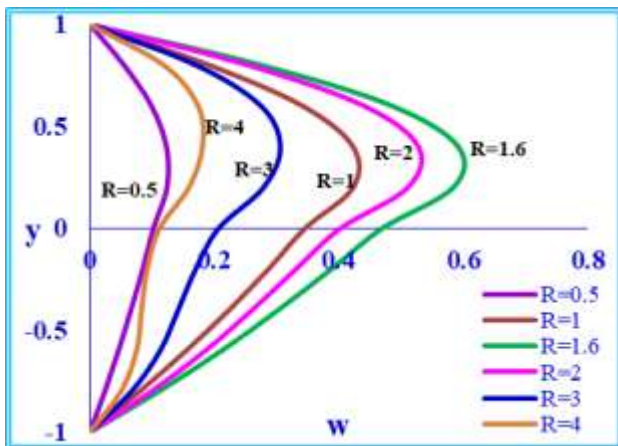


Fig.3: Secondary velocity for different values of R.

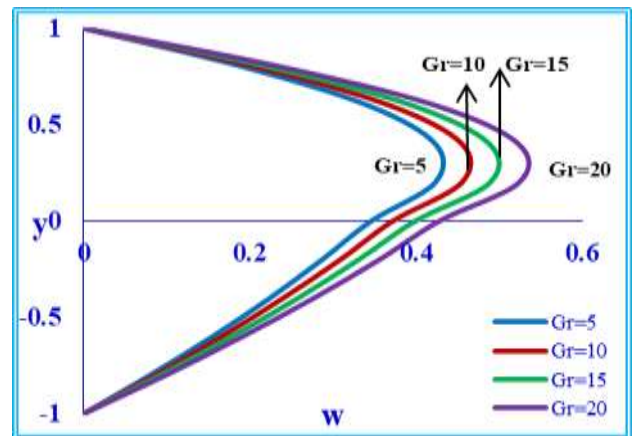


Fig. 7: Secondary velocity for various values of Gr.

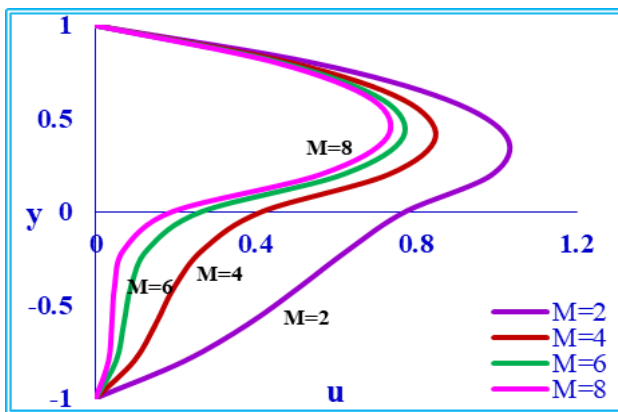


Fig. 4: Primary velocity for various values of M.

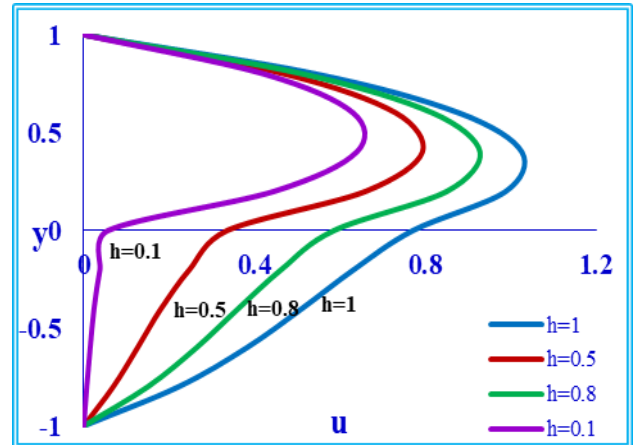


Fig. 8: Primary velocity for various values of h.

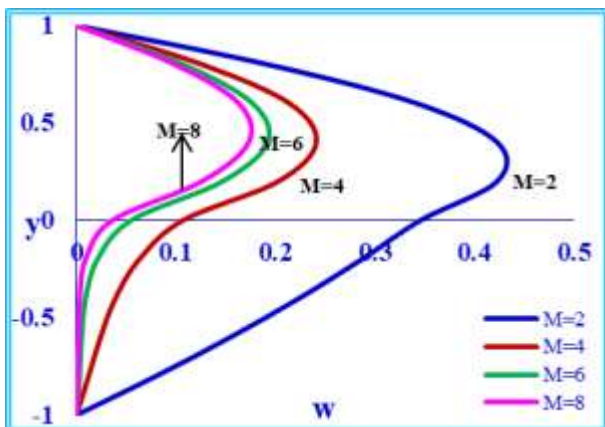


Fig. 5: Secondary velocity for various values of M.

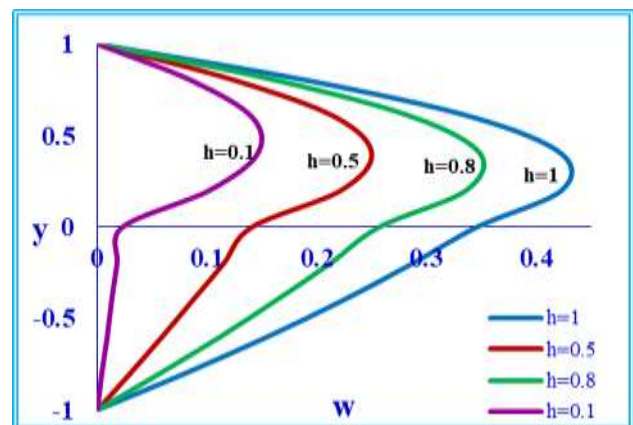


Fig. 9: Secondary velocity for various values of h.

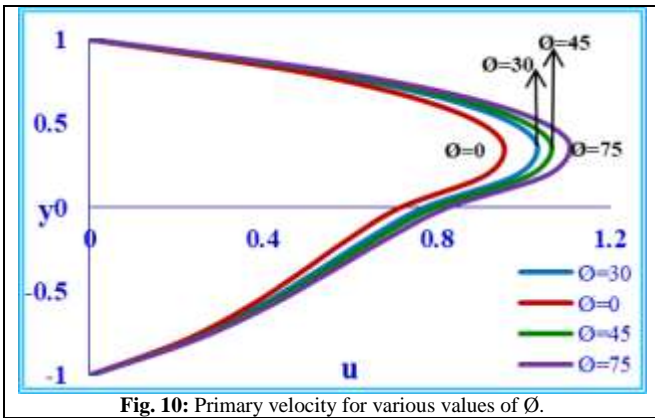


Fig. 10: Primary velocity for various values of Φ .

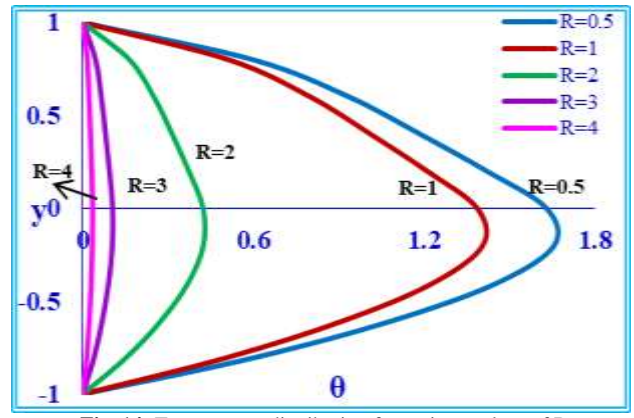


Fig. 14: Temperature distribution for various values of R .

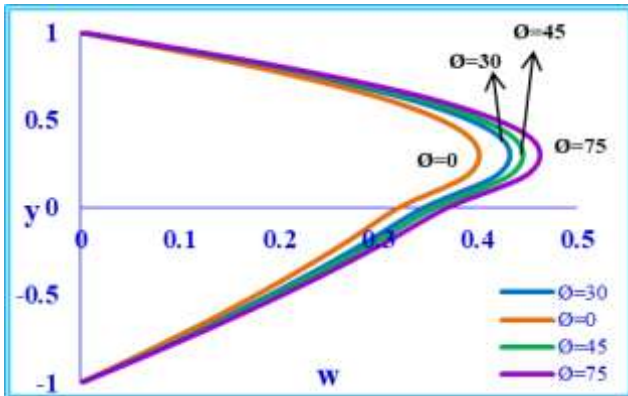


Fig. 11: Secondary velocity for various values of Φ .

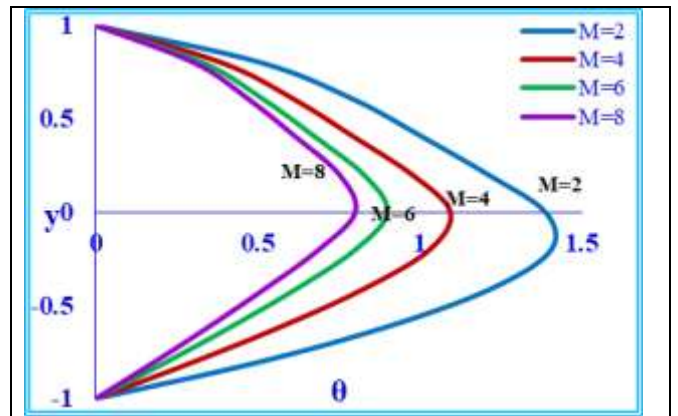


Fig. 15: Temperature distribution for various values of M .

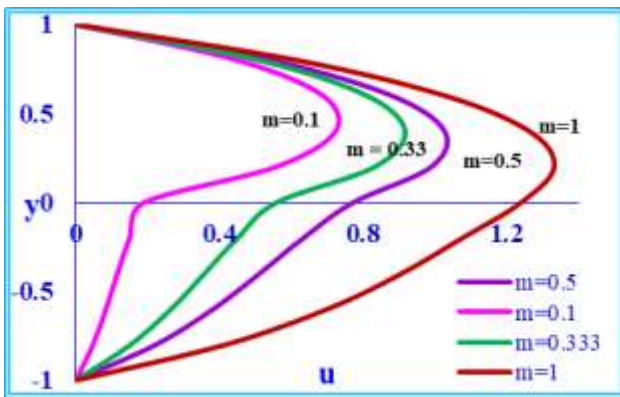


Fig. 12: Primary velocity for various values of m .

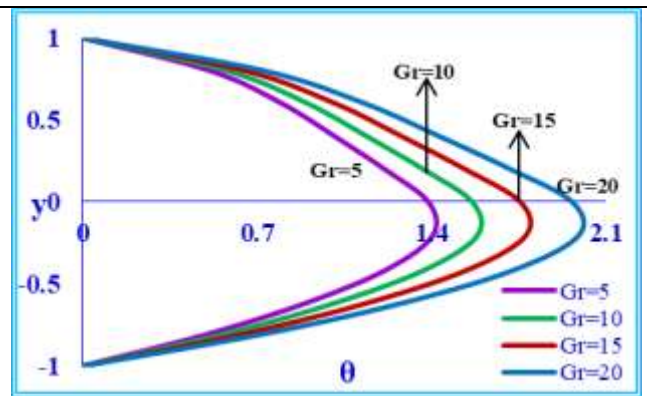


Fig. 16: Temperature distribution for various values of Gr .

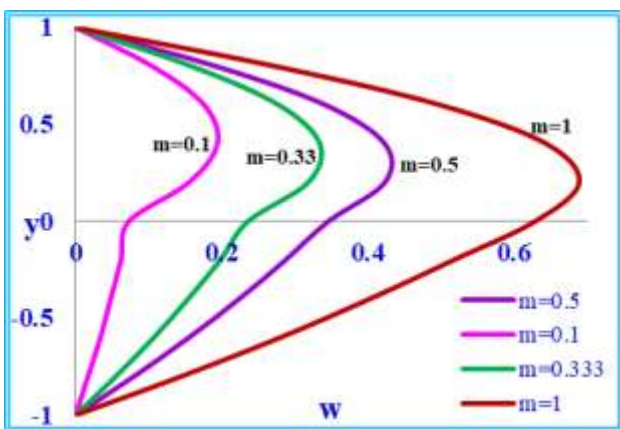


Fig. 13: Secondary velocity for various values of m .

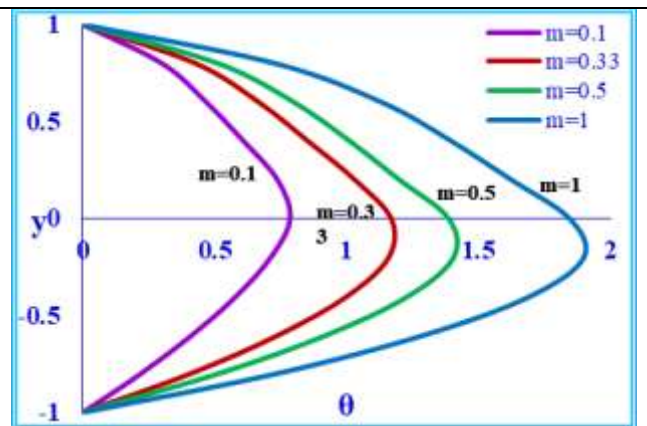


Fig. 17: Temperature distribution for various values of m .

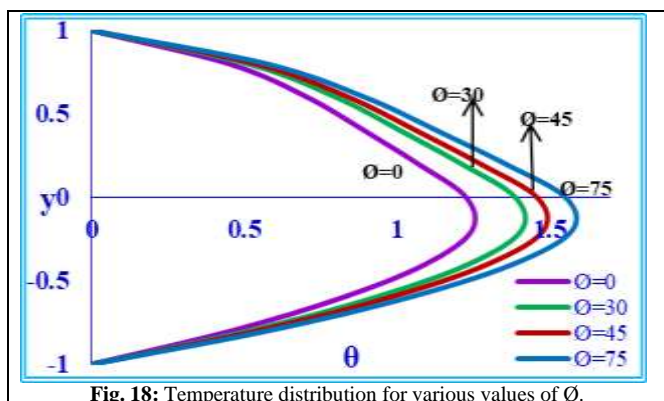


Fig. 18: Temperature distribution for various values of \emptyset .

6. References

- [1] Shail R (1973), On laminar two-phase flow in a magneto- hydrodynamics, International journal of Engineering Science 11, 1103-1108.
- [2] Seth GS, Raj Nandkeolyar & Ansari MS (2010), Hartmann flow in a rotating system in the presence of inclined magnetic field with hall effects, Tamkang Journal of Science & Engineering, Vol.13, No.3, 243-252.
- [3] Lohrasbi J & Sahai V (1989), Magneto-hydrodynamic heat transfer in two-phase flow between parallel plates, Applied Scientific Research 45, 53-66.
- [4] Malashetty MS & Leela V (1992), Magnetohydrodynamic heat transfer in two phase flow, International Journal of Engineering Science 30, 371-377.
- [5] Linga Raju T & Murty PSR (2006), Hydromagnetic two-phase flow and heat transfer through two parallel plates in a rotating system, Journal of Indian Academy of Mathematics, Vol.28, No.2, 343-360.
- [6] Chauhan DS & Rastogi P (2012), Heat transfer effects on rotating MHD couette flow in a channel partially filled by a porous medium with hall current, Journal of Applied Science & Engineering, Vol.15, No.3, 281-290.
- [7] Abdul Mateen (2013), Magneto-hydrodynamic flow and heat transfer of two immiscible fluids through a horizontal channel, International Journal of Current engineering and Technology 3, 1952-1956.
- [8] Abdul Mateen (2014), Transient magneto-hydrodynamic flow of two immiscible fluids through a horizontal channel, International Journal of Engineering Research, Vol.3, No.1, 13-17.
- [9] Malashetty MS & Umavathi JC (1997), Two- phase Magnetohydrodynamic Flow and Heat transfer in an inclined channel, International Journal of Multiphase flow, Vol.23, No.3, 545-560.
- [10] Malashetty MS, Umavathi JC & Prathap Kumar J (2001), Convective Magnetohydrodynamic two Fluid Flow and Heat transfer in an Inclined Channel, Heat and mass transfer Vol.37, No.2-3, 259-264.
- [11] Simon Daniel & Shagaiya Daniel Y (2013), Convective flow of two immiscible fluids and heat transfer with porous along an inclined channel with pressure gradient, Research Invents: International Journal of Engineering and Science, Vol.2, No.4, 12-18.
- [12] Sri Ramachandra Murty P & Balaji Prakash G (2014), Heat Transfer Aspects on Rotating MHD two-phase convective Flow through an Inclined Channel in the Presence of Electric Field, Physical Science International Journal, Science Domain international 4, 1260-1279.
- [13] Sri Ramachandra Murty P & Balaji Prakash G (2014), MHD Two-Fluid Flow and Heat transfer between two inclined parallel plates in a rotating system, International Scholarly Research Notices, Hindawi Publishing Corporation, 11
- [14] Sri Ramachandra Murty P & Balaji Prakash G (2016), Magneto-hydrodynamic two-fluid flow and heat transfer in an inclined channel containing porous and fluid layers in a rotating system, Maejo International Journal of Science and Technology, Vol.10, No.1, 25-40.